JOURNAL OF MATERIALS SCIENCE 13 (1978) 739–749

Epitaxial growth of antimony electrodeposits on oriented single crystal surfaces of gold and silver

M. LAZZARI, L. PERALDO BICELLI, B. RIVOLTA
Centro di Studio sui Processi Elettrodici del C.N.R. Istituto di Chimica Fisica, Elettrochimica e Metallurgia del Politecnico di Milano, Italy

A. LA VECCHIA
Cattedra di Siderurgia, Istituto di Meccanica applicata alle macchine, Università di Genova, Italy

The epitaxial growth of antimony electrodeposits, obtained at 25 and 50° C from a chloride bath on single crystal cathodes of gold and silver, oriented along the (1 0 0), (1 1 0) and (1 1 1) crystallographic planes, has been studied by electron diffraction. Current densities ranging from 10 to 1000 A m^{-2} and thicknesses between 1 and 50 μm have been investigated. The gold substrate was found to be the more favourable to the formation of oriented crystalline deposits. A tendency to form amorphous antimony was observed on the silver substrate, especially at 25° C. The monocrystalline deposits on (1 0 0) and (1 1 1) planes of gold and silver were oriented with their (1 0 0) plane parallel to the substrate, and the deposits on the (1 1 0) plane of gold and silver with their (1 1 0) and ($\bar{1}$ 1 0) planes parallel to the substrate. The orientation relationships between parallel directions of the deposit and substrate have been determined. The results are discussed in terms of the work of formation of variously oriented nuclei on amorphous substrates, the symmetry elements in the deposit–substrate interface region and the mismatch along the more densely packed parallel directions.

1. Introduction

Much research work has recently been done on the structure and orientation of thin metal layers formed by epitaxy on various oriented single crystal surfaces of different materials, due to growing interest in possible applications. Much research has also been done on the epitaxy of relatively thick deposits, which may be investigated by high energy electron diffraction (RHEED) and X-ray diffraction techniques [1]. The deposits were obtained both by condensation from vapour (often on non-metallic single crystal surfaces, such as mica, alkali halides, etc.) and by electrocrystallization.

In the present work the structure, orientation and morphology of deposits obtained on cathodes either of the same or different nature have been investigated. Antimony was also taken into consideration as its behaviour in this field is not well known. Investigations were made both into the structural aspects of electrolytic antimony deposits on single crystal surfaces of antimony [2], and the kinetic–electrochemical aspects related to the electrodeposition process [3].

The main aim of the present research is to extend the previous investigations to antimony deposits on extraneous single crystal cathodes with respect to the conditions of epitaxial growth and the orientation relationships between the deposit and the substrate.

Gold and silver substrates were investigated to avoid chemical displacement occurring in the absence of applied current. In future research, copper will also be considered. These metals

possess a f c c structure (O_h^5) which is different from that of antimony (rhombohedral, $D_{3\,d}^{5}$; nevertheless, as angle α approaches 90°, to a first approximation the lattice of antimony may be likened to a pseudo-f c c lattice*.

Deposits of thicknesses between 1 and 50 μm were made at current densities between 10 and 1000 A m^{-2} and at temperatures of 25 and 50° C. Most of the deposits were obtained from a chloride bath as in previous work; it was also considered useful to carry out some experiments with a citrate bath as frequently used in galvanic techniques. There is little literature on this subject, but we are aware of a paper discussing antimony deposits obtained by high vacuum deposition on single crystal potassium chloride substrates, orientated along the (1 0 0) plane and examined by transmission electron diffraction and microscopy [4].

2. Experimental

The gold and silver single crystals were prepared from 4N pure metals using a modified Bridgman technique. The method of cutting the single crystals in order to obtain discs of about 20 mm in diameter, oriented along the (1 0 0), (1 1 0) and (1 1 1) crystallographic planes, is reported in a previous paper [5]. Polishing of the various substrates, to achieve surfaces free from work-hardened layers, is performed under the following conditions:

gold – electrolytic polishing in 70 g l^{-1} KCN solution and 15 g l^{-1} Seignette salt solution; voltage 15 V, current density 150 A dm^{-2}, duration 2 min, stainless steel cathode; rinsing in 1M $HClO_4$ solutions;

silver – chemical polishing in 0.2 M KCN solution with the addition of a few drops of 36% H_2O_2 (by volume), followed by rinsing with a 0.2 M KCN solution.

The solutions used for deposition were as follows: (a) 0.5M $SbCl_3$ + 3M HCl; (b) 52.4 g l^{-1} Sb_2O_3, 149.8 g l^{-1} potassium citrate, 179.7 g l^{-1} citric acid. The solutions were prepared from analytical reagents and doubly distilled water and were further treated with activated carbon. Solution (b) was only used to prepare deposits on the silver substrate at 50° C.

The electrolytic cell and apparatus were the same as those described previously [5]. The measurements were carried out using the galvanostatic technique. In order to avoid displacement reactions in the absence of applied current, the electrodes were polarized cathodically as soon as they were dipped in the solution. After each deposition, the samples were rinsed in a solution HCl and doubly distilled water in the ratio 1:1. The structure of the deposits, the orientation and epitaxial relationships with the substrate were investigated by the RHEED technique (Trüb Täuber apparatus, voltage 50 kV, camera length 50 cm).

3. Results

The results for the deposits obtained on the various single crystal surfaces, under different conditions of temperature, current density and thickness, are reported in Table I. In Table II the orientation relationships between parallel directions of the deposit and substrate, interatomic distances and relative per cent mismatch are given. It should be noticed that after parallelism has been assigned to a pair of directions, there is not always parallelism for the other pairs of directions owing to the pseudo-cubic structure of antimony. In Table II the pairs of directions showing a deviation from parallelism are marked by an asterisk.

3.1. Deposits on gold

The monocrystalline antimony deposits were oriented with their (1 0 0) planes parallel to the substrate (1 0 0) and (1 1 1) planes, and with their (1 1 0) and ($\bar{1}$ 1 0) planes parallel to the substrate (1 1 0) plane. The relationship to the (1 0 0) plane is always found to be that indicated by α in Table II (Figs. 1a and b). In one case, namely for deposits obtained at 50° C, 100 A m^{-2} and thicknesses of 50 μm, a second relationship (indicated by β), was noticed alongside the first orientation relationship. This second relationship corresponds to the iso-orientation between deposit and substrate.

In all the diffraction patterns obtained with the electron beam parallel to the [0 0 1] direction of the antimony, the diffraction spots were double and symmetrically arranged with respect to the [1 0 0] direction of the substrate (see Fig. 1b). This result is a consequence of antimony's rhombohedral structure, as may be deduced from Fig. 2; the two pseudo-cubic crystallites have a face in common, and therefore two crystallographic axes in common, one of which is the [0 0 1] axis. The

*The lattice parameters of the substrates and deposit are: Au, a = 4.0704 Å; Ag, a = 4.0778 Å; Sb, a = 6.221 Å; α = 87° 42′.

TABLE I Orientation of antimony deposits from a chloride bath on the (1 0 0), (1 1 0) and (1 1 1) faces of gold and silver single crystals.

Substrate	Temperature (° C)	Current density ($A m^{-2}$)	Thickness (μm)	Growth faces		
				(1 0 0)	(1 1 0)	(1 1 1)
Au	25	100	1	(1 0 0)*	(1 1 0), ($\bar{1}$ 1 0)	(1 0 0)
	50	100	1	(1 0 0)	(1 1 0), ($\bar{1}$ 1 0)	(1 0 0)
			10	(1 0 0)	(1 1 0), ($\bar{1}$ 1 0), [$\bar{1}$ 1 2]†	(1 0 0)
			20	(1 0 0)	[$\bar{1}$ 1 2]	–
			50	(1 0 0)	–	–
		1000	1	(1 0 0)	(1 1 0), ($\bar{1}$ 1 0)	(1 0 0)
			10	(1 0 0)	(1 1 0), ($\bar{1}$ 1 0)	(1 0 0),
			50	(1 0 0)	(1 1 0), ($\bar{1}$ 1 0)	(1 0 0)
Ag	25	25	2	amorphous	amorphous	(1 0 0)
			5	–	amorphous	–
		100	1	–	–	amorphous, (1 0 0)
	50	10	1	(1 0 0)	(1 1 0), ($\bar{1}$ 1 0)	(1 0 0)
		25	2	(1 0 0)	(1 1 0), ($\bar{1}$ 1 0)	(1 0 0)
		100	1	–	–	(1 0 0)

*Plane of the deposit parallel to the substrate surface
†Texture axis of the deposit.

TABLE II Orientation relationships, interatomic distances and corresponding mismatches between parallel directions.

Substrate orientation	Antimony deposit orientation		Orientation relationship between parallel directions	Interatomic distances along the considered directions (Å)		Mismatch (%)
				Deposit	Substrate	
(1 0 0)	(1 0 0)		[0 1 1] Sb* ∥ [0 1 $\bar{1}$] Au, Ag	6.22	2.88 × 2	8.0
		α	[0 1 1] Sb* ∥ [0 1 0] Au, Ag	4.49	4.07	10.2
			[0 0 1] Sb ∥ [0 1 1] Au, Ag	6.22	2.88 × 2	8.0
			[0 $\bar{1}$ 1] Sb* ∥ [0 0 1] Au, Ag	4.31	4.07	5.8
		β	[0 $\bar{1}$ $\bar{1}$] Sb ∥ [0 1 1] Au	4.31	2.88 × 2	25.2
			[0 1 0] Sb* ∥ [0 1 0] Au	6.22	4.07	52.8
			[0 $\bar{1}$ 1] Sb ∥ [0 1 1] Au	4.49	2.88 × 2	22
			[0 0 1] Sb* ∥ [0 0 1] Au	6.22	4.07	52.8
(1 1 0)	(1 1 0)		[$\bar{1}$ 1 1] Sb* ∥ [$\bar{1}$ 1 $\bar{2}$] Au, Ag	10.63	4.99 × 2	6.5
			[0 0 1] Sb ∥ [$\bar{0}$ 0 1] Au, Ag	6.22	2.88 × 2	8.0
			[1 $\bar{1}$ 1] Sb* ∥ [1 1 2] Au, Ag	10.63	4.99 × 2	6.5
			[1 $\bar{1}$ 0] Sb ∥ [0 0 1] Au, Ag	4.31	4.07	5.8
	($\bar{1}$ 1 0)		[1 1 1] Sb* ∥ [$\bar{1}$ 1 $\bar{2}$] Au, Ag	11.20	4.99 × 2	12.2
			[0 0 1] Sb ∥ [$\bar{1}$ 1 0] Au, Ag	6.22	2.88 × 2	8.0
			[$\bar{1}$ $\bar{1}$ 1] Sb* ∥ [$\bar{1}$ 1 2] Au, Ag	10.63	4.99 × 2	6.5
			[$\bar{1}$ $\bar{1}$ 0] Sb* ∥ [0 0 1] Au, Ag	4.49	4.07	10.2
(1 1 1)	(1 0 0)	α	[0 1 1] Sb ∥ [$\bar{1}$ 1 0] Au, Ag	4.31	2.88 × 2	25.2
			[0 1 1] Sb ∥ [$\bar{1}$ $\bar{1}$ 2] Au, Ag	4.49	4.99	10.0
		β	[0 1 0] Sb* ∥ [$\bar{1}$ 1 0] Au, Ag	6.22	2.88 × 2	8.0
			[0 0 1] Sb ∥ [$\bar{1}$ $\bar{1}$ 2] Au, Ag	6.22	4.99	25.2

*Directions not strictly parallel to each other.

other pairs of corresponding faces are not parallel with respect to one another and therefore not strictly parallel, nor perpendicular to the substrate surface. The deviations are very small; they have been purposely exaggerated in Fig. 2.

Figs. 1c, d, and e show the RHEED patterns of epitaxial antimony deposits on the (1 1 0) plane. The double positioning due to the presence of the two crystallographic planes (1 1 0) and ($\bar{1}$ 1 0) parallel to the substrate having very close interplanar distances (equal to 4.485 Å and 4.309 Å, respectively), may be clearly seen.

When the thickness was increased, the deposits tended towards disorientation with a [$\bar{1}$ 1 2]

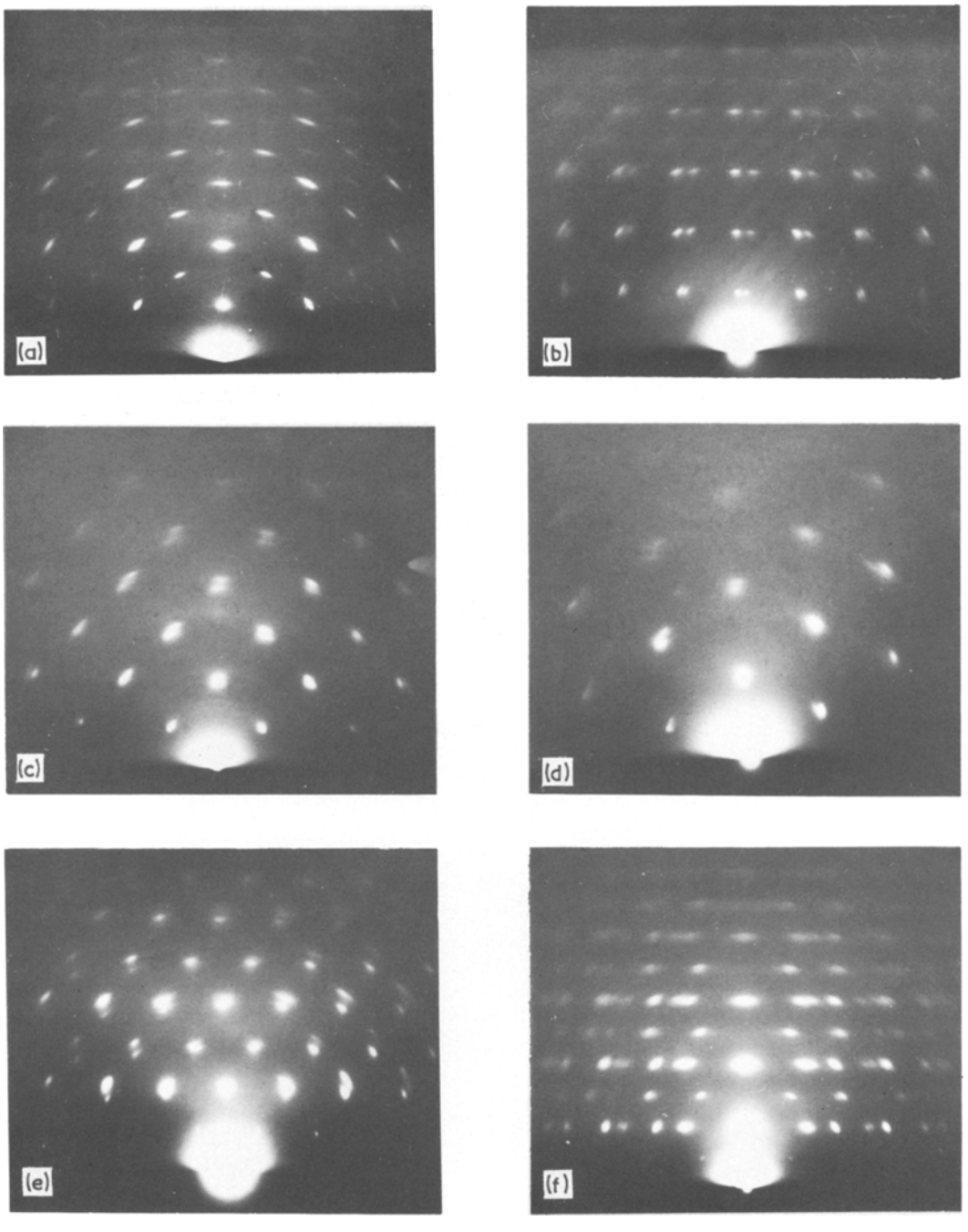

Figure 1 RHEED patterns of antimony deposits on gold substrates: (a) and (b) (1 0 0) face; (c), (d) and (e) (1 1 0) face; (f) (1 1 1) face (50° C). (a) 100 A m^{-2}, 1 μm; beam along [0 1 0] Au. (b) 1000 A m^{-2}, 10 μm; beam along [0 1 1] Au. (c) 100 A m^{-2}, 1 μm; beam along [$\bar{1}$ 1 0] Au. (d) 1000 A m^{-2}, 1 μm; beam along [$\bar{1}$ 1 $\bar{2}$] Au. (e) 1000 A m^{-2}, 1 μm; beam along [0 0 1] Au. (f) 100 A m^{-2}, 30 μm; beam along [$\bar{1}$ $\bar{1}$ 2] Au.

texture axis. Furthermore, it was not possible to obtain diffraction patterns for some samples at higher current densities with thicknesses of 10 and 50 μm. This would be in agreement with the tendency, which increases with current density, to form amorphous antimony, which can hide the diffraction pattern of the crystalline metal.

The monocrystalline deposits obtained on the (1 1 1) plane were always oriented with the (1 0 0)

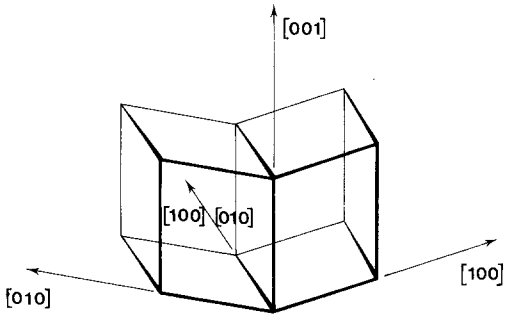

Figure 2 Double positioned rhombohedral crystallites of antimony on a (1 0 0) gold face. The deviation from 90° of the pseudo-cube angles is strongly exaggerated.

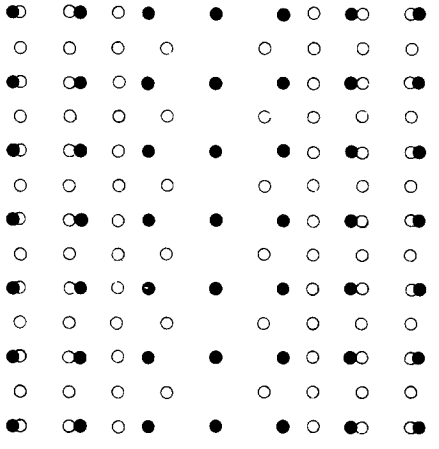

Figure 3 Interpretation of the diffraction pattern shown in Fig. 1f. ○ beam along [0 1 1] Sb ∥ [$\bar{1}$ $\bar{1}$ 2] Au, • beam along [0 0 1] Sb ∥ [$\bar{1}$ $\bar{1}$ 2] Au.

plane parallel to the substrate, and usually gave two different orientation relationships at the same time, such relationships being indicated by α and β in Table II. Fig. 1f shows a typical diffraction pattern whose interpretation is given in Fig. 3. Fig. 1f also shows the double positioning of the diffraction spots for the deposits on the (1 1 1) plane, which is due to orientation β, in which the electron beam is approximately parallel to the [0 0 1] direction of antimony.

On increasing the thickness of the deposit, the diffraction spots become arcs, indicating a gradual disorientation of the deposits. When the thickness of the deposits is increased at the highest current density, the second orientation relationship tended to disappear so that diffraction patterns for thicknesses equal to or greater than 10 μm revealed the presence of the α relationship only. As already observed for deposits on the(1 1 0) plane, diffraction patterns were weak for certain samples of greater thicknesses obtained at 1000 A m^{-2}, indicating the presence of amorphous antimony in this case as well.

The deposits on the three planes were generally uniform, compact and adherent; when examined by metallographic microscopy, they were revealed as granular structures (Fig. 4a) with geometric forms, especially those obtained at the higher current densities (Fig. 4b). This is in agreement with the shape of the diffraction spots.

3.2. Deposits on silver

The deposits obtained at 25° C on the (1 0 0) plane

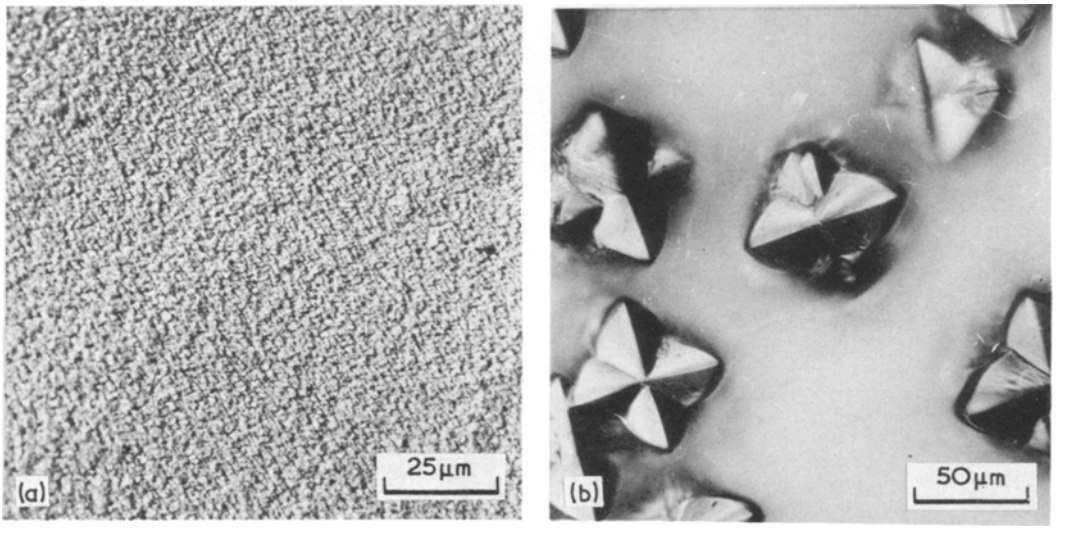

Figure 4 Micrographs of antimony deposits on a (1 0 0) gold face (50° C). (a) 100 A m^{-2}, 1 μm; (b) 1000 A m^{-2}, 10 μm.

did not give diffraction patterns, due to the presence of amorphous metal, while the deposits obtained at 50° C on the same substrate were always monocrystalline with the (1 0 0) plane oriented parallel to the substrate and with the α orientation relationship indicated in Table II. This relationship was identical to that observed in all cases for gold (Figs. 5a and b).

The same considerations made for deposits on the (1 0 0) plane are valid for deposits on the (1 1 0) plane. At 25° C the deposit was amorphous, while at 50° C it was monocrystalline, with the (1 1 0) plane, and also, less frequently, the ($\bar{1}$ 1 0) plane parallel to the substrate, the orientation relationships being identical to those observed for gold (Fig. 5c).

The deposits on the (1 1 1) plane were also monocrystalline at 25° C. As in the case of gold, the (1 0 0) plane was parallel to the substrate with two different orientation relationships which were always observed simultaneously. When the current density was increased, a tendency towards amorphous antimony formation was observed. At 50° C, the tendency to give monocrystalline deposits even at 100 A m^{-2} was noticed. The plane parallel to the substrate was still the (1 0 0) plane with the previously mentioned orientation relationships (Fig. 5d).

As in the case of deposits on gold, the double positioning of the diffraction spots was observed. There were no special features in the morphology of the deposits. They were generally uniform, compact, with no growth forms, and sometimes shiny, especially on the (1 1 0) plane in the presence of the amorphous metal.

For the deposits obtained from the citrate bath (at a temperature of 50° C, current density 25 A m^{-2} and thickness 0.5 μm), only in few cases, and only on the (1 1 0) plane, was it possible to reveal an oriented crystalline deposit. Here the (1 1 0) plane, which was slightly disoriented, was parallel to the substrate and the orientation

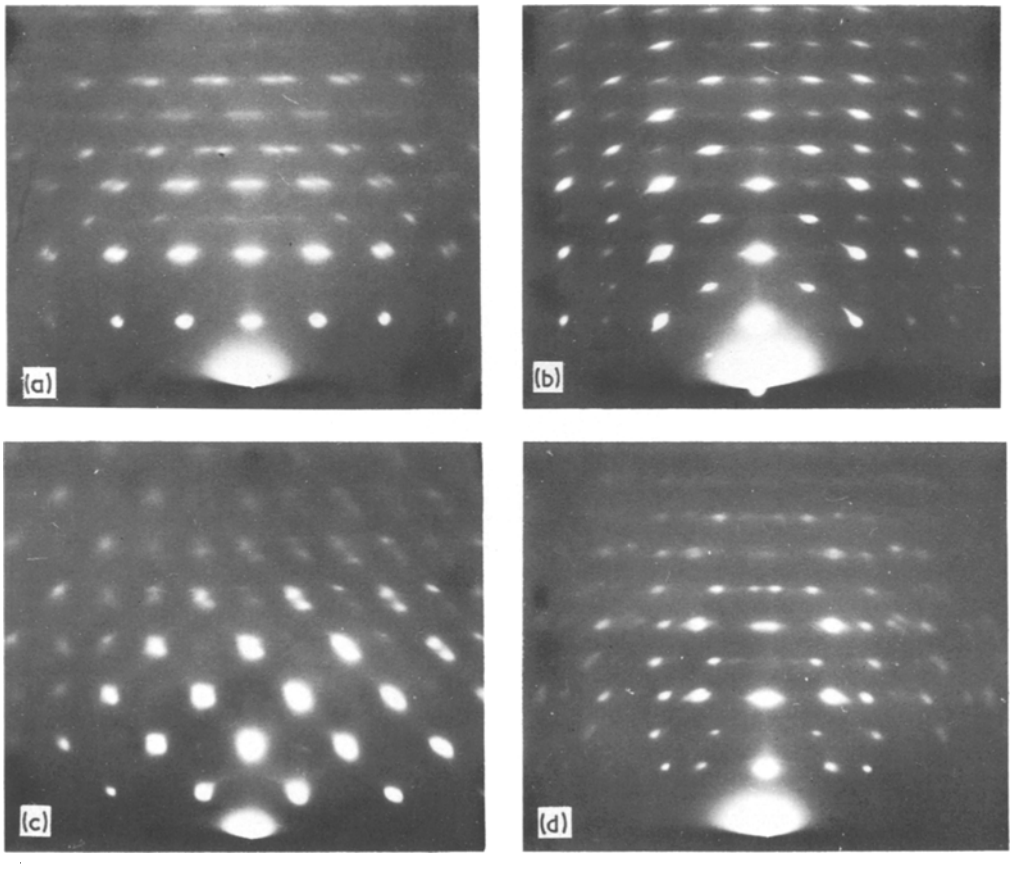

Figure 5 RHEED patterns of antimony deposits on silver substrates: (a) and (b) (1 0 0) face; (c) (1 1 0) face; (d) (1 1 1) face (50° C). (a) 10 A m^{-2}, 1 μm; beam along [0 1 1] Ag. (b) 25 A m^{-2}, 2 μm; beam along [0 1 0] Ag. (c) 10 A m^{-2}, 1 μm; beam along [$\bar{1}$ 1 0] Ag. (d) 100 A m^{-2}, 1 μm; beam along [$\bar{1}$ $\bar{1}$ 2] Ag.

relationships were identical to those observed for deposits from the chloride bath. The $(\bar{1}\,1\,0)$ plane was not observed. The deposits were of a shiny and uniform appearance.

4. Discussion of the results

The type of growth observed in electrodeposited metals on single crystal substrates is governed by the influence of the orientation of the substrate, and by the influence of the deposition conditions (current density, temperature, type of bath, etc.). The first influence favours the epitaxial growth, while when the second prevails, nuclei tend to form oriented along the crystallographic plane having the lower work of formation; this can also bring about the formation of polycrystalline deposits with preferred orientations. Whether one influence or the other dominates depends on energetic, dimensional and valency factors [6]. The influence of the substrate tends to dominate when the forces of interaction between two different types of metal atoms are of the same magnitude, or even greater than the forces existing between atoms of the same type, when the relative difference between atomic radii of the metals forming the deposit and the substrate is small, and lastly, when, according to Hume-Rothery, a high valency metal is deposited on a low valency metal (as occurs in the cases considered in this paper).

Another condition which favours epitaxial growth occurs when the substrate is already oriented along the plane for which the work of formation of nuclei is small. The calculation of the work of formation on an amorphous cathode of two-dimensional nuclei oriented along various crystallographic planes of fcc metals [7, 8] and hcp metals [8, 9] has been performed by Pangarov, who also showed that such work depends on the overvoltage of the electrodeposition process. Hence different results are predicted for metals having the same structure, but which, for example, are normal or inert in the kinetic-electrochemical sense*.

In the electrodeposition on extraneous cathodes, as the values of overvoltage are rarely known, reference is generally made to the overvoltage of the metal deposited on a cathode of the same metal. If antimony is likened to a metal of pseudo-fcc crystal structure, owing to its property of being an intermediate metal [3], the plane for which the work of nucleation is the least is the (1 0 0) plane, and the work of formation of nuclei along (1 1 0) is not appreciably different from work of formation of nuclei along (1 0 0).

The results obtained on gold and silver agree, therefore, with predictions. In fact, on substrates (1 0 0) and (1 1 0) planes, the orientation of the substrate is the decisive factor in the formation of one or other of the two types of nuclei, both being favoured by the conditions of deposition. Owing to the considerable difference in the atomic radii of the deposit and of the substrates, iso-oriented growth is rarely observed. On the contrary, the influence of the conditions of deposition seems to dominate on the substrate (1 1 1) planes, hence nuclei are formed which are oriented along the plane having the least work of nucleation. Furthermore, as antimony has a rhombohedral structure, and unlike nuclei oriented along the (1 0 0) plane, nuclei oriented along the (1 1 0) and $(\bar{1}\,1\,0)$ planes have a different structure, the latter are both always observed even when the former seems, at times, to be favoured.

As regards the orientation of the deposit on the substrate, it has been found [10] that it generally is such as to provide a plane at the deposit–substrate interface† having the maximum possible symmetry (i.e. with the highest number of elements of symmetry), independent of the mismatch along parallel directions. Usually, however, for a particular symmetry of this plane, the orientation relationship which implies only a small mismatch along the directions of high atomic density has been observed [6]. This has also been found for the deposits considered in this research.

In order to illustrate the orientation relationships and the elements of symmetry of the various superimposed planes, representations were made as in Figs. 6 to 8. For reasons of clarity, the double positioning of the antimony crystallites on the (1 0 0) and (1 1 1) planes was omitted from the figures.

*The so-called normal, intermediate or inert metals are characterized in electrodeposition by an exchange of ions which is fast, intermediate or slow respectively, and therefore by small, intermediate or high overvoltage, for the same value of current density.

†This plane is formed by the projection of the atoms of the two superimposed planes.

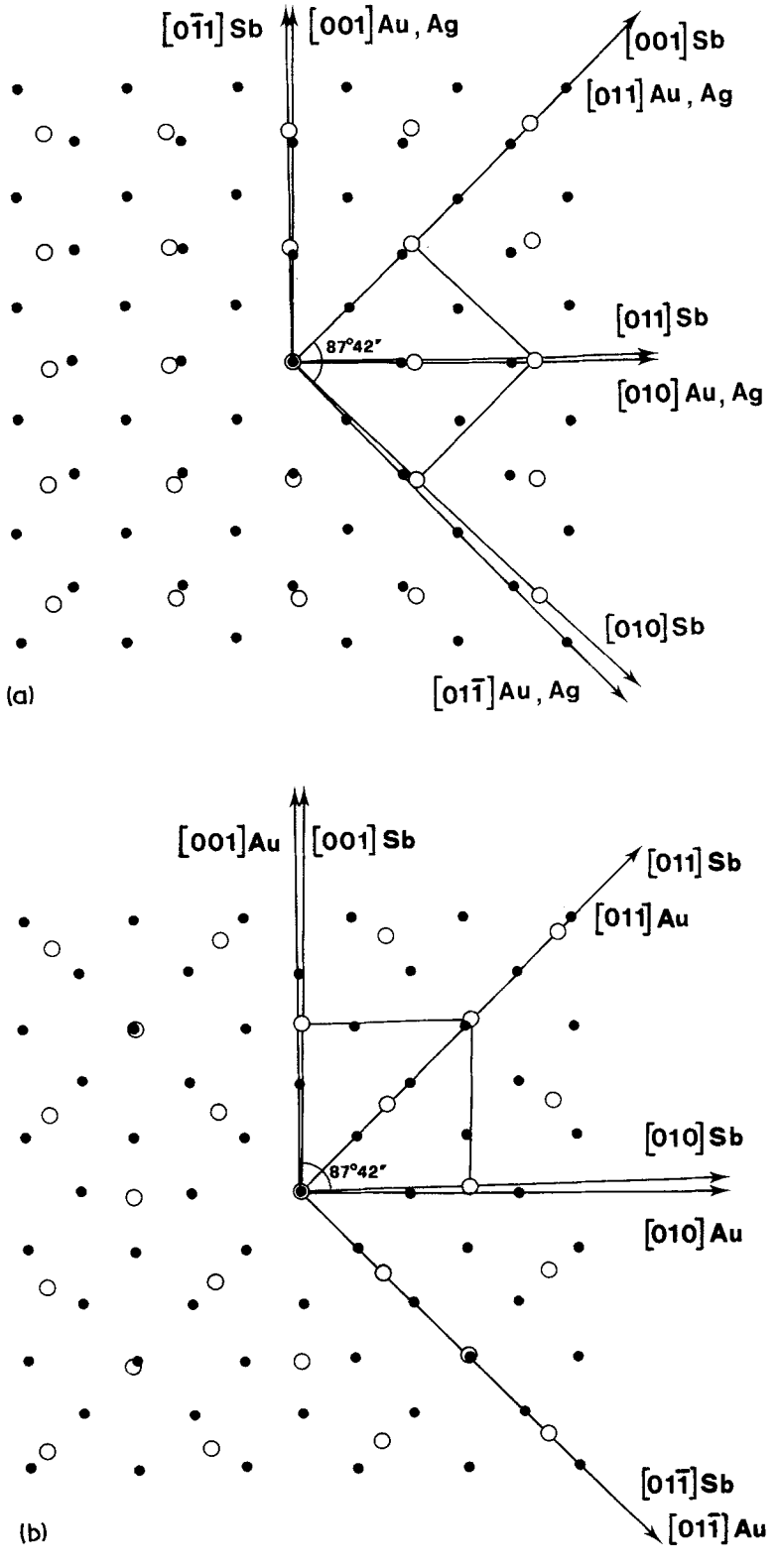

Figure 6 Positions of the antimony atoms of the (1 0 0) plane superimposed on the atoms of the (1 0 0) plane of substrate. ○ Sb; ● Au, Ag. (a) [0 0 1] Sb ‖ [0 1 1] Au, Ag. (b) [0 1 1] Sb ‖ [0 1 1] Au.

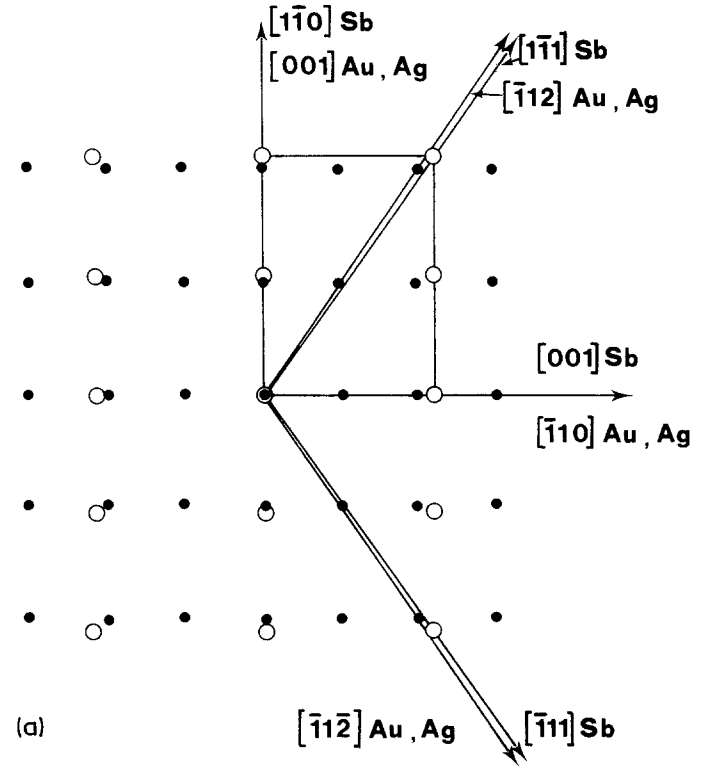

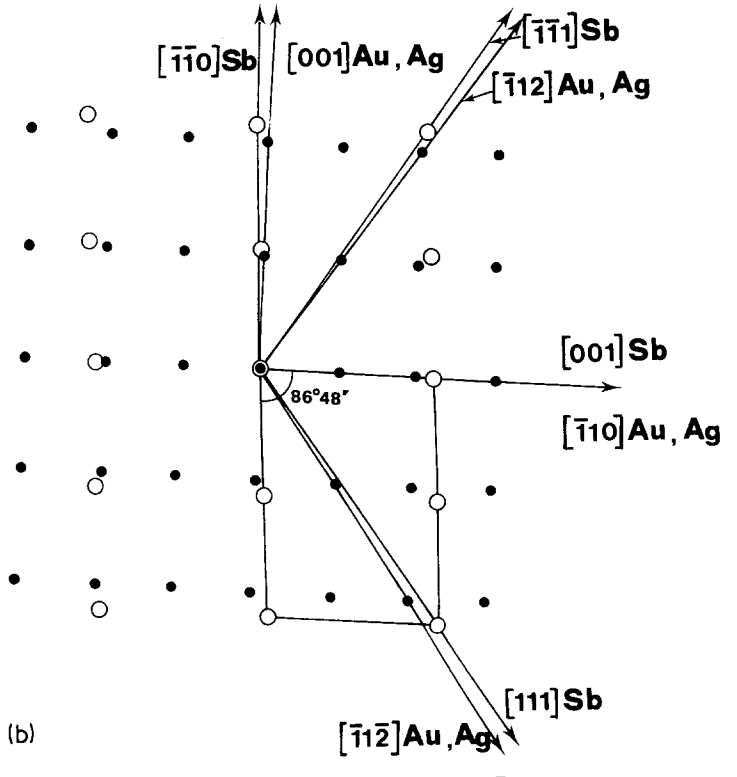

Figure 7 Positions of the antimony atoms of the (1 1 0) plane (a) and ($\bar{1}$ 1 0) plane (b) superimposed on the atoms of the (1 1 0) plane of the substrate. ○ Sb; ● Au, Ag.

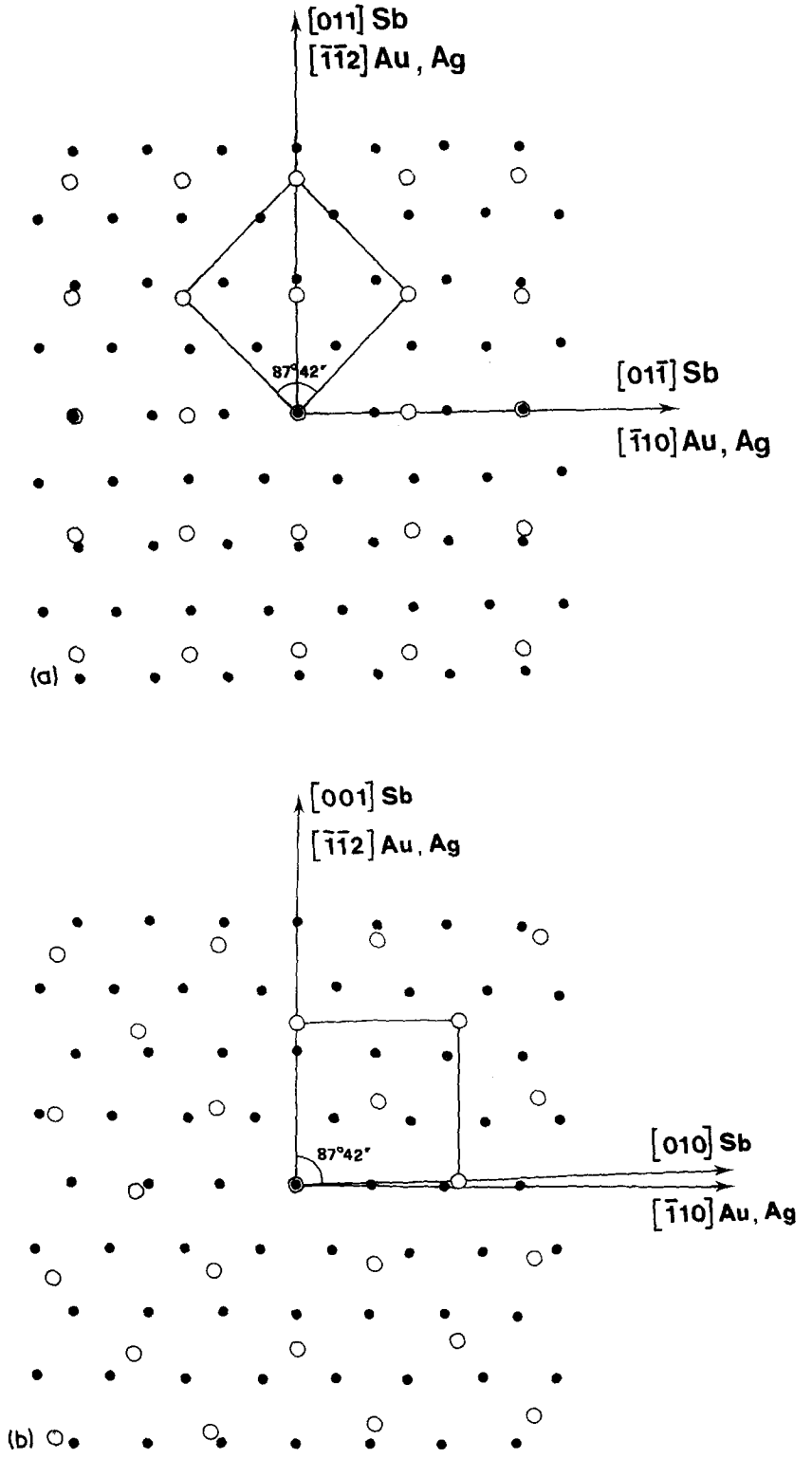

Figure 8 Positions of the antimony atoms of the (1 0 0) plane superimposed on the atoms of the (1 1 1) plane of substrate ○ Sb; • Au, Ag. (a) [0 1 1] Sb ∥ [1̄ 1̄ 2] Au, Ag. (b) [0 0 1] Sb ∥ [1̄ 1̄ 2] Au.

Figs. 6a and b represent the distribution of the atoms of the antimony deposit on the (1 0 0) plane of gold and silver where the orientation relationships, indicated by α and β in Table II, occur. Assuming antimony to have a fcc structure, the two types of relative orientation involve the maximum possible symmetry of the interphase plane (p4mm two-dimensional space group); furthermore the first of the two orientations shows a particularly low mismatch (5.8%) between the most densely packed direction [0 $\bar{1}$ 1] of antimony and the [0 0 1] direction of the substrate.

Analogous considerations are applicable for the deposits on the (1 1 0) plane of gold and silver. The corresponding orientations which are represented in Figs. 7a and b, when the (1 1 0) or ($\bar{1}$ 1 0) plane is parallel to the substrate respectively, involve a very low mismatch (6 to 10%) between the most densely packed directions. This mismatch is certainly much less than in the case of iso-orientation, but, although this iso-orientation gives rise an interphase plane with the same maximum symmetry (p2mm two-dimensional space group), it has never been observed. Furthermore, from the figures it may be seen how the more frequently observed (1 1 0) nucleus, at least in the case of silver, adapts itself better to the substrate structure as it has angles of 90° and a lower mismatch.

On the (1 1 1) planes, however, the two orientation relationships presented in Figs. 8a and b, usually occur simultaneously; this is in agreement with the fact that they involve the same maximum symmetry of the interphase plane (c2mm two-dimensional space group) and do not show significant differences in mismatching between the parallel directions. Only under conditions of high current density and thickness, at which only the gold deposits are still crystalline, is the preferred orientation the one which implies parallelism between the most densely packed directions. This is a condition which has often been found [6].

It can therefore be concluded that the results obtained are in agreement with predictions based upon; (a) the work of nucleation, (b) the symmetry of the interphase plane, and (c) the mismatch along parallel directions.

References

1. J. W. MATTHEWS, "Epitaxial Growth", Parts A and B (Academic Press, New York, 1975).
2. G. POLI and B. RIVOLTA, *Electrochim. Metall.* **3** (1968) 7.
3. G. POLI, B. RIVOLTA and A. LA VECCHIA, *Atti, Accad. Naz. Lincei, Mem., Classe Sci. Fis., Mat. e Nat., Sez. II* **29** (1960) 345.
4. K. BAHADUR and K. CHAUDHARY, *Appl. Phys. Lett.* **15** (1969) 277.
   W. SCHUZ, *Phys. Stat. Sol.* **A1** (1970) K81.
5. R. PIONTELLI, *Electrochim. Metall.* **1** (1966) 5.
6. L. PERALDO BICELLI and B. RIVOLTA, *Ann. Chim.* (Rome) **66** (1976) 467.
7. N. A. PANGAROV, *Electrochim. Acta* **7** (1962) 139.
8. N. A. PANGAROV, *J. Electroanal. Chem.* **9** (1965) 70.
9. N. A. PANGAROV, *Electrochim. Acta* **9** (1964) 721.
10. E. FERRONI and M. COCCHI, *Atti Accad. Naz. Lincei, Mem., Classe Sci. Fis., Mat. e Nat., Sez. II* **5** (1958) 117.

Received 30 May and accepted 13 September 1977.